Influence of annealing temperature on visible-light photocatalytic activities of Ag_3PO_4 particulates synthesized using CH_3COOAg as a precursor*

SUI Mei-rong (隋美蓉)[1]**, **SUN Ya-nan** (孙亚男)[2], **GU Xiu-quan** (顾修全)[2], **SHI Mei-lin** (时梅林)[1], **WANG Yong** (王永)[1], **and LIU Lin-lin** (刘琳琳)[1]

1. School of Medical Imaging, Xuzhou Medical University, Xuzhou 221004, China

2. School of Materials Science and Engineering, China University of Mining and Technology, Xuzhou 221116, China

(Received 3 February 2018; Revised 20 March 2018)

©Tianjin University of Technology and Springer-Verlag GmbH Germany, part of Springer Nature 2018

Ag_3PO_4 microparticles (MPs) were prepared through a facile chemical precipitation route and using silver acetate (AgAc) as metal salt. The effect of annealing temperature (T_a) and time (τ_a) on the actual photocatalytic (PC) activity of Ag_3PO_4 MPs is investigated. The optimal annealing parameters are T_a of 400 °C and τ_a of 90 min. The enhanced PC activity by annealing at 400 °C is ascribed to the increase of electron mobility. Besides, an Ag_3PO_4 photoelectrode was fabricated through a drop-coating deposition route, which demonstrates a photocurrent density of 80 μA/cm^2 and acceptable stability. The n-type conduction behavior of Ag_3PO_4 is verified by a Mott-Schottky (M-S) plot.

Document code: A **Article ID:** 1673-1905(2018)04-0291-5

DOI https://doi.org/10.1007/s11801-018-8020-2

Recently, Ag_3PO_4 has become one of the most promising photocatalytic (PC) materials among all metal oxide photocatalysts due to its relatively small band gap (~2.4 eV) to permit an efficient visible light harvesting[1-3]. It can achieve the quantum efficiency (*QE*) of up to 90% for O_2 evolution at wavelength of about 420 nm[4]. As a comparison, the QE of TiO_2 or other semiconductors is only 20%—30%. However, Ag_3PO_4 still suffers from a challenge of poor stability in the practical applications. This kind of material is easily photocorroded and decomposed to weakly active Ag, which is accompanied with a color change from yellow to dark. Besides, it is difficult to construct an Ag_3PO_4 photoelectrode for photoelectrochemical (PEC) applications due to the poor adhesion or stability. As demonstrated by $BiVO_4$, WO_3 and α-Fe_2O_3, the PEC cell is an efficient way for utilizing the solar energy[5,6].

Up to now, a number of reports have been focused on how to enhance the performance of Ag_3PO_4. The formation of a heterojunction with other components is a common strategy. For instance, Samal et al[7] synthesized a visible light driven, direct Z-scheme photocatalyst based on the reduced graphene oxide (RGO)-Ag_3PO_4 heterostructure, leading to a high H_2 evolution rate of 3 690 μmol·h^{-1}·g^{-1}. Wan et al[8] reported the preparation of a Z-scheme $CaIn_2S_4/Ag_3PO_4$ nanocomposite which exhibits a superior PC performance in removal of NO, and the PC oxidation efficiency can reach 83.61%. However, in the most of previous reports, $AgNO_3$ was used as the metal salt for synthesis of Ag_3PO_4.

So far, much attention has been paid towards the PC properties of Ag_3PO_4, while few studies are focused on its PEC application due to a challenge in constructing a photoelectrode. Early in 2011, Bi et al[9] reported the preparation of $AgBr/Ag_3PO_4$ electrodes through a facile drop-coating method, leading to a photocurrent density of 40 μA/cm^2 under visible light irradiation. Lin et al[10] facilitated a ZnO nanorod array (NRA) decorated with $Ag@Ag_3(PO_4)_{1-x}$ nanoparticles (NPs), leading to a considerable photocurrent density of ~3.2 mA/cm^2 under solar irradiation by using a two-electrode cell, and the actual solar-to-electricity was calculated to be 2%. Wu et al[11] fabricated a Ag/Ag_3PO_4 core/shell layer photoelectrode by anodizing the electrodeposited Ag nanoplate arrays, achieving a photocurrent density of ~0.25 mA/cm^2 under an applied bias of +0.5 V versus the saturated calomel electrode (SCE), while the O_2 evolution was observed clearly. So far, there are few reports on the Mott-Schottky (M-S) plots of Ag_3PO_4, which is an efficient method to identify the conduction type of this material.

In this work, we synthesized the sphere-like Ag_3PO_4 microparticles (MPs) by using AgAc as the metal ionic source, and investigate the effect of annealing temperature (T_a) and time (τ_a) on the visible-light PC activity. Further, a photoelectrode was fabricated by depositing the Ag_3PO_4 MPs onto a fluorine doped SnO_2 coated (FTO) substrate. The M-S analyses are carried out to

* This work has been supported by the Natural Science Foundation of Xuzhou City (No.KC14SM088), and the Natural Science Fund for Colleges and Universities of Jiangsu Province (Nos.15KJB430031 and 16KJB310019).

** E-mail: smr2012@xzhmu.edu.cn

confirm the n-type characteristic of Ag_3PO_4.

All chemical reagents used in this work, including AgAc, disodium hydrogen phosphate (Na_2HPO_4) and ethanol, are analytical grade without further purification or other treatment.

Sphere-like Ag_3PO_4 MPs were prepared by a facile ion-change method, which is similar to one of our previous reports[12] except using AgAc instead of $AgNO_3$. Briefly, 100 mL Na_2HPO_4 aqueous solution (0.01 mol/L) was added dropwise into 5 mL AgAc aqueous solution (0.06 mol/L) under a vigorous stirring. After stirring for another 0.5 h in dark, the yellow precipitates produced from that chemical reaction were collected by centrifuging, then washed with water and ethanol in turn for several times. Finally, the Ag_3PO_4 MPs were dried at 40 °C in vacuum for 12 h, followed by annealing at 100—500 °C for 30—120 min.

The X-ray diffraction (XRD) was carried out to characterize the structure of the Ag_3PO_4 MPs on a D8 Advance Bruker diffractometer with Cu Kα irradiation. The surface morphology was examined by a field emission scanning electron microscopy (FESEM, S-4800, Hitachi, Japan). The diffusion absorption spectra were collected by an ultraviolet-visible (UV-vis) spectrophotometer (Varian Cary 300).

The PC performance was evaluated by degrading the Rhodamine B (RhB) under visible light irradiation, which was provided by a 150 W halogen lamp made in Beijing Institute of Optoelectronic Technology. Prior to the measurements, 0.1 g samples were dispersed in 100 mL RhB solution (10 mg/L), and then stirred in the dark for 30 min to reach the adsorption equilibrium. During the irradiation time, 3 mL suspensions were removed at certain time, and then centrifuged with rate of 10 000 r/min for 3 min to separate the MPs from the solution. The concentration of RhB aqueous solution was then determined by measuring the absorbance at 553 nm using a UV-vis spectroscopy (UV-2500PC, Shimadzu).

Prior to the PEC measurements, 0.006 g Ag_3PO_4 powders were ground and dispersed in 0.1 mL terpilenol to form a paste, which was then scrape-coated onto the substrates to obtain a film. Then, the as-deposited Ag_3PO_4 films were calcined at 400 °C for 1 h. The PEC measurements were performed in an electrochemical workstation (CHI660E, Shanghai, China) with a standard three-electrode setup, which employed a Pt mesh as the counter electrode, SCE as the reference electrode and Ag_3PO_4 film as the working electrode, respectively. The electrolyte was 0.1 mol/L Na_2SO_4 aqueous solution, while a 300 W Xe lamp equipped with a filter (λ>420 nm) was employed to provide a visible light irradiation of 100 mW/cm^2. The current density versus time (*J*-*t*) curves were collected under a chopped visible light irradiation and a bias of 0.6 V versus SCE, while the M-S plots were recorded in dark at a frequency of 1 kHz.

Fig.1 shows the surface morphology of Ag_3PO_4 MPs before and after annealing in air at 400 °C and 500 °C for 30 min. The as-synthesized MPs display a sphere-like shape and an average size of ~200 nm. After annealing, a serious particle aggregation occurs, leading to larger and interconnected grains, being consistent with our previous report[12]. Besides, it is also found that the color of Ag_3PO_4 powders gets brighter after annealing at 400 °C, which is associated with the stronger reflection over the long wavelength band (λ>500 nm).

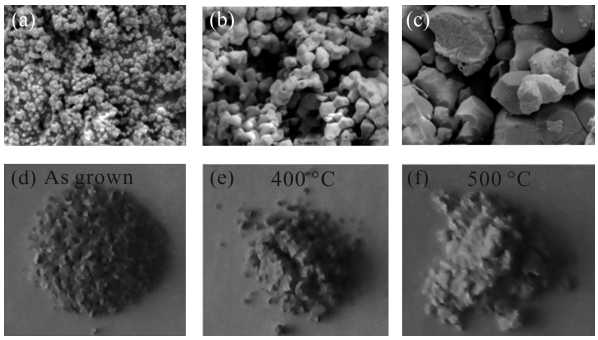

Fig.1 SEM images of (a) as-grown Ag_3PO_4 sample and Ag_3PO_4 samples annealed at (b) 400 °C and (c) 500 °C; Digital photographs of (d) as-grown Ag_3PO_4 samples and Ag_3PO_4 samples annealed at (e) 400 °C and (f) 500 °C

Fig.2(a) compares the XRD patterns of Ag_3PO_4 MPs before and after annealing. All the diffraction peaks can be assigned to the cubic-phase Ag_3PO_4 in terms of JCPDS No.06-0505. There is not any peak from Ag or Ag_2O, indicative of a good purity. Besides, the intensities of these peaks are enhanced, while no any changes in the peak positions are observed after annealing. Fig.2(b) shows the reflection spectra of the as-synthesized and 400 °C annealed Ag_3PO_4 MPs. The samples can reflect the photons with λ>500 nm, which is consistent with their colors. And also, there aren't obvious differences in the light harvesting capabilities of the samples before and after annealing. The fundamental bandgap of Ag_3PO_4 is estimated to be ~2.28 eV.

Fig.2(c) and (d) compare the PC activities of Ag_3PO_4 MPs annealed at various temperatures. It is found clearly that the as-grown Ag_3PO_4 MPs can degrade 97% of RhB in 6 min under visible light irradiation. However, after 100—350 °C annealing, the PC activity decreases sharply due to the rapidly increased particle sizes. Surprisingly, the PC activity is restored to the initial state (as-grown) with increasing T_a to 400 °C, although the surface area is reduced a lot. It is speculated that the enhancement of PC activity might benefit from the enhanced carrier mobility due to the interconnection of the MPs. However, when T_a reaches 450 °C or 500 °C, the PC activity decreases again, which can be attributed to a rapid increase of the average particle size as indicated in Fig.1(c) (over 6 μm). It is noteworthy that 500 °C is close to the melt point of Ag_3PO_4 (~540 °C).

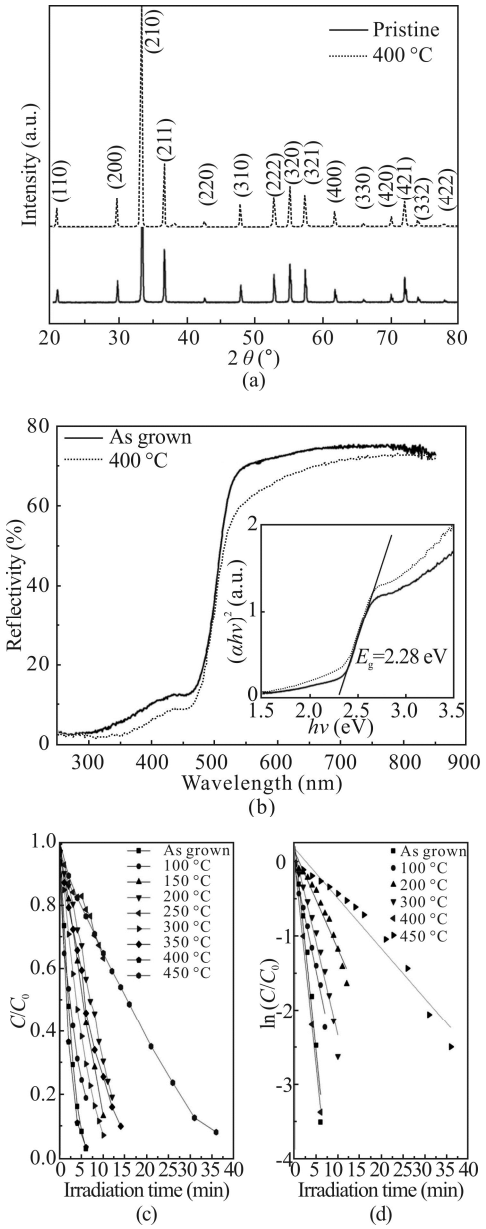

Fig.2 (a) XRD patterns, (b) UV-vis diffusion spectra, (c) C/C_0 versus time and (d) ln(C/C_0) versus time curves of the Ag_3PO_4 samples annealed at different temperatures (The inset of (b) displays $(ahv)^2$ versus photonic energy relation for calculating E_g of Ag_3PO_4.)

Fig.3 displays the PC recyclabilities of Ag_3PO_4 MPs before and after 400 °C annealing. Although there aren't obvious differences in the PC activity of two samples due to a competition of the surface area and carrier mobility, the PC stability is enhanced significantly after the annealing process. In detail, during the fourth circle, the as-grown sample can degrade 89 % of RhB in 8 min, while the sample after 400 °C annealing can degrade 95 % of RhB in 7 min. The enhanced PC stability might be related with a suppression of the photocorrosion effect, owing to the lowered contact area of Ag_3PO_4 MPs with water.

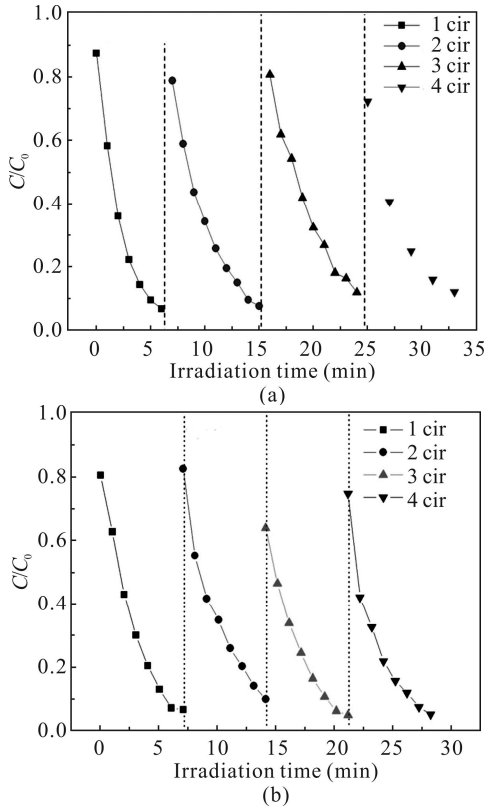

Fig.3 Recyclabilities of RhB photodegradation of Ag_3PO_4 powders (a) before and (b) after 400 °C annealing for 30 min

Fig.4(a) displays the influence of τ_a on the PC activity of Ag_3PO_4 MPs. It is demonstrated that the PC activity can be enhanced efficiently by extending τ_a. Herein, the sample after 90 min annealing displays the highest PC activity, which can degrade 96% of RhB in 4 min. It suggests that the photo-corrosion is suppressed efficiently by reducing the specific surface area (i.e., reducing the contact chance of Ag_3PO_4 surface with water). As can be seen in Fig.4(b), there aren't obvious changes in the average grain sizes by comparing the (210) peak widths (located around 33.3°, from 0.166° to 0.168°), suggesting that the enhanced PC activity might be associated with the other factors except the specific surface area. Fig.5 shows the FESEM images of the Ag_3PO_4 MPs annealed at various τ_a. It is noted that a few thin Ag nanoparticles (NPs) can be formed uniformly on the large-size MPs with increasing τ_a, which might be beneficial for enhancing the charge carrier separation, leading to a better PC activity. However, when τ_a reaches 120 min, excess Ag NPs might affect the light harvesting, resulting in a slight reduction of PC activity again.

Fig.6 displays the cross-section SEM images of a porous Ag_3PO_4 film (annealing at 400 °C) which is used for PEC measurements. It is observed that the film displays a thickness of ~50 μm and is made up of many Ag_3PO_4 MPs. Through annealing, these MPs are packed together to form a compact thick film, which might be beneficial to enhance the charge carrier transport.

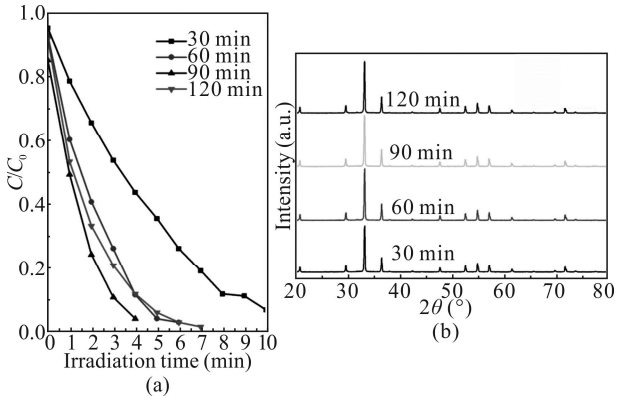

Fig.4 (a) C/C_0 versus time curves and (b) XRD patterns of Ag_3PO_4 samples annealed at 400 °C for various τ_a values from 30 min to 120 min

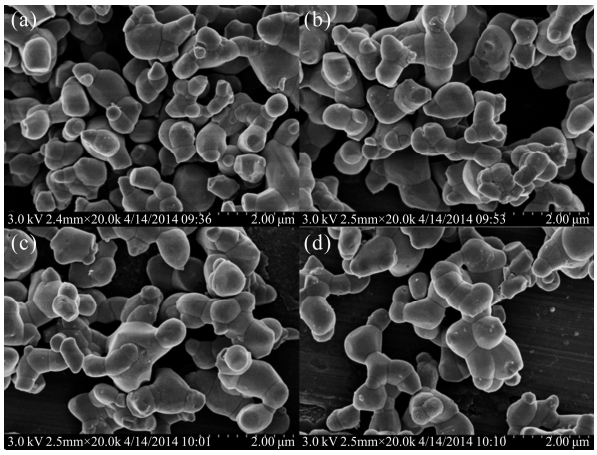

Fig.5 FESEM images of the 400 °C sintered Ag_3PO_4 samples undergoing different τ_a of (a) 30 min, (b) 60 min, (c) 90 min and (d) 120 min

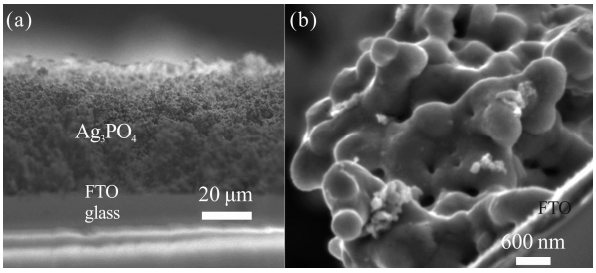

Fig.6 Cross-section SEM images of Ag_3PO_4 electrodes made up of MPs and underwent a 400 °C sintering for 1 h with (a) low and (b) high magnification rate

Fig.7(a) and (b) show the transient photocurrent response of a porous Ag_3PO_4 film. Although this film is a little thick, a photocurrent density of ~80 μA/cm^2 can be reached, suggesting that the photo-excited electrons can be collected efficiently by the FTO layer. Besides, the photocurrent can be also stable for at least 300 s, making it feasible to carry out an electrochemical impedance measurement (including the M-S plots). Even after a 2 000 s irradiation, the photocurrent still remains ~50% of the initial value, implying that the photocorrosion is suppressed efficiently. Fig.7(c) displays a typical M-S plot of the porous Ag_3PO_4 films after 400 °C annealing. The positive slope value indicates that Ag_3PO_4 is an n-type semiconductor, while its flat-band potential (V_{fb}) is about −0.18 V versus SCE. This value is significantly more positive than TiO_2 (~0.7 V versus SCE), which is consistent with its more positive conduction band edge (CBE) than TiO_2.

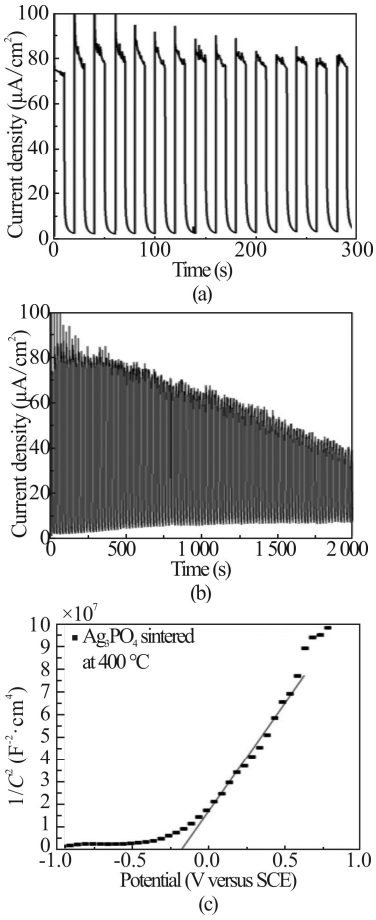

Fig.7 Typical *J-t* curves under a chopped visible-light irradiation of Ag_3PO_4 powder electrodes sintered at 400 °C for 1 h with (a) short duration of 300 s and (b) long duration of 2 000 s; (c) An M-S plot of Ag_3PO_4 powder electrodes obtained at 0.0 V versus SCE in dark

Ag_3PO_4 MPs were synthesized through a facile chemical precipitation method, followed by annealing to enhance the crystalline quality and construct a porous film. We also investigate the influence of annealing time on the actual PC activity of Ag_3PO_4 MPs. It is found that the highest PC performance can be achieved in the Ag_3PO_4 samples after annealing at 400 °C for 90 min. Such an enhancement is attributed to a more efficient carrier transport resulting from the interconnection of these Ag_3PO_4 MPs. Moreover, an Ag_3PO_4 photoanode is fab-

ricated through annealing the drop-deposited films at 400 °C. The n-type conduction type is versified by the M-S plot. We hope that this study is helpful for understanding the PC phenomenon occurring in Ag_3PO_4 or other semiconductor photocatalysts or photoelectrodes.

References

[1] H.B. Wu, H.H. Hng and X.W. Lou, Adv. Mater. **24**, 2567 (2012).

[2] X. Xu, C. Randorn, P. Efstathiou and J.T.S. Irvine, Nat. Mater. **11**, 595 (2012).

[3] D.J. Martin, G. Liu, S.J.A. Moniz, Y. Bi, A.M. Beale, J. Ye and J. Tang, Chem. Soc. Rev. **44**, 7808 (2015).

[4] D.J. Martin, N. Umezawa, X. Chen, J. Ye and J. Tang, Energy Environ. Sci. **6**, 3380 (2013).

[5] T.W. Kim and K.S. Choi, Science **343**, 990 (2014).

[6] C. Du, X. Yang, M.T. Mayer, H. Hoyt, J. Xie, G. McMahon, G. Bischoping and D. Wang, Angew. Chem. Int. Ed. **52**, 12692 (2013).

[7] A. Samal, D. P. Das, K. K. Nanda, B. K. Mishra, J. Das and A. Dah, Chem-Asian J. **11**, 584 (2015).

[8] S. Wan, M. Ou, Q. Zhong and S. Zhang, New J. Chem. **42**, 318 (2018).

[9] Y. Bi, H. Hu, S. Ouyang, G. Lu, J. Cao and J. Ye, Chem. Commun. **48**, 3748 (2012).

[10] Y. Lin, Y. Hsu, Y. Chen, S. Wang, J. T. Miller, L. Chen and K. Chen, Energy Environ. Sci. **5**, 8917 (2012).

[11] Q. Wu, P. Diao, J. Sun, D. Xu, T. Jin and M. Xiang, J. Mater. Chem. A **3**, 18991 (2015).

[12] S. Zhang, X. Gu, Y. Zhao and Y. Qiang, Mater. Sci. Eng. B **201**, 57 (2015).